Supplementary material

Based on the cleavage kinetic scheme (**Figure S3**) and steady-state approximations, Han et al. [1] we obtain the Michaelis constant K_m and maximum cleavage rate $V_{\max}$ as follows:

$$K_m = \frac{\left(k_2\left(k_{-3}+k_p\right)+k_{-1}\left(k_{-2}+k_{-3}+k_p\right)\right)\left(1+\frac{k_4}{k_{-4}}\right)}{k_1\left(k_2+k_{-2}+k_{-3}+k_p\right)+k_3\frac{k_4}{k_{-4}}\left(k_{-2}+k_2+k_{-1}\right)} \quad [S1]$$

and

$$V_{\max} \approx \frac{k_p\left(k_1k_2+\frac{k_4}{k_{-4}}k_3(k_{-2}+k_{-1})\right)[E]_{total}}{k_1\left(k_2+k_{-2}+k_{-3}+k_p\right)+k_3\frac{k_4}{k_{-4}}\left(k_{-2}+k_2+k_{-1}\right)} \quad [S2]$$

Here $[E]_{total}$ is the total enzyme concentration. Experimental studies have shown that for heterotrimer, $K_m = 0.8 \pm 0.08$ μ. Surprisingly, the homotrimer has a similar Michaelis constant, $K_m = 0.9 \pm 0.2$ μm. Therefore, the smaller cleavage rate of homotrimer results entirely from the smaller maximum cleavage rate $V_{\max}$.

We use $k_{-1} = 5 \times 10^{-3}\ \mathrm{s}^{-1}$ and $k_p = 1\ \mathrm{s}^{-1}$ in our analysis because experimental results show that k_{-1}~$5 \times 10^{-3}\ \mathrm{s}^{-1}$ [2-4] and $k_p = 0.11$~$11\ \mathrm{s}^{-1}$ [3-5].. Note that k_{-3} should be within the same order of k_{-1}, we have $k_p \gg k_{-3}$. Because atomistic simulations show that the homotrimer cleavage site is thermally stable, we assume $\frac{k_4}{k_{-4}} \ll 1$ for homotrimers. These assumptions lead to

$$K_m(\text{homotrimer}) = \frac{k_{-1}}{k_1}\left(\frac{\left(1+\frac{k_p}{k_{-1}}K_U\right)}{1+K_U}\right) \quad [S3]$$

and

$$k_{cat}(\text{homotrimer}) = \frac{V_{\max}(\text{homotrimer})}{[E]_{total}} \approx \frac{k_pK_U}{1+K_U} \quad [S4]$$

Here we have used $K_U = \frac{k_2}{k_{-2}+k_{-3}+k_p}$. We use experimental results by Han et al. [1] ($K_m(\text{homotrimer}) = 0.9$ μm, and $k_{cat}(\text{homotrimer}) = 0.007\ \mathrm{s}^{-1}$) to solve for unknown variables in Eq. S3 and Eq. S4.

The heterotrimer is thermally unfolded within nanoseconds and previous studies observe $\frac{k_4}{k_{-4}} \approx 1$ at room temperature [6], thus we are motivated to study the rate equations without assuming $\frac{k_4}{k_{-4}} \ll 1$ and neglecting all terms proportional to $\frac{k_4}{k_{-4}}$ at the first step. We assume that k_{-2} is relatively small compared to k_p and k_{-1}, which is reasonable since we do not expect the MMP would be likely to fold the unfolded collagen into triple helical structure and we expect once MMP binds a vulnerable conformation of collagen it would likely cleave it. Based on these assumptions, we rearrange Eq. S1 and Eq. S2 into

$$K_m = \frac{k_{-1}}{k_1}\left(\frac{\left(1+\frac{k_p}{k_{-1}}K_U\right)\left(1+\frac{k_4}{k_{-4}}\right)}{1+\left(1+\frac{k_3}{k_1}\frac{k_4}{k_{-4}}\right)K_U+\frac{k_3}{k_1}\frac{k_4}{k_{-4}}\frac{k_{-1}}{k_p}}\right) \quad [S5]$$

and

$$k_{cat} = \frac{V_{\max}}{[E]_{total}} \approx \frac{k_p K_U\left(1+\frac{k_3}{k_1}\frac{k_4}{k_{-4}}\right)}{1+\left(1+\frac{k_3}{k_1}\frac{k_4}{k_{-4}}\right)K_U+\frac{k_3}{k_1}\frac{k_4}{k_{-4}}\frac{k_{-1}}{k_p}} \quad [S6]$$

Note that the remaining unknowns are $\frac{k_3}{k_1}$ and $\frac{k_4}{k_{-4}}$. All other parameters, K_U, k_{-1}, and k_p have been determined experimentally for homotrimers. It is worth noting that $\frac{k_3}{k_1}$ represents the ratio of the rate enzyme binds to the vulnerable state of collagen compared to the rate enzyme binds to the native state of collagen. Previous studies have shown that the local conformation of the cleavage site may provide a recognition signal for MMPs [2, 7, 8]. Thus, we expect that $k_3 > k_1$. Because there are no experimental results for the values of $\frac{k_3}{k_1}$ or $\frac{k_4}{k_{-4}}$, we study the values of $0 < \frac{k_3}{k_1} < 100$ and $10^{-6} < \frac{k_4}{k_{-4}} < 1$. We consider an extreme case that $\frac{k_4}{k_{-4}}$ is the only different parameter between heterotrimer and homotrimer to study how the thermal stability of collagen affects the degradation rate.

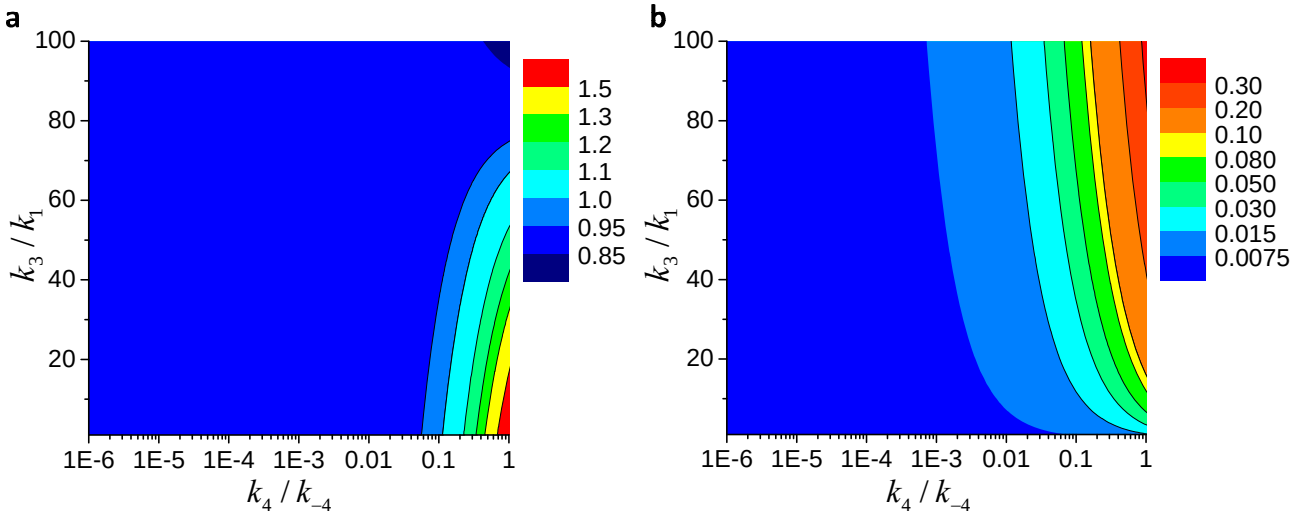

Figure S1 | Analysis of the Michaelis constant K_m (Eq. S5) and degradation rate k_{cat} (Eq. S6). (a) K_m (b) k_{cat}

The results (**Figure S1**) show that within the range of the values we studied, there is not much change of K_m which is consistent with the experimental finding that $K_m(\text{heterotrimer}) \approx K_m(\text{homotrimer})$. When $\frac{k_4}{k_{-4}}$ is small enough, the K_m remains constant. If both $\frac{k_4}{k_{-4}}$ and $\frac{k_3}{k_1}$ are large, a slightly smaller value of K_m is obtained which is likely the case found in experiments that $K_m(\text{heterotrimer}) = 0.8\ \mu\text{m}$ which is slightly smaller compared to $K_m(\text{homotrimer}) = 0.9\ \mu\text{m}$. On the other hand, large $\frac{k_4}{k_{-4}}$ and small $\frac{k_3}{k_1}$ would result in a larger value of K_m.

Interestingly, the results of degradation rate reveal that increasing $\frac{k_4}{k_{-4}}$, i.e. decreasing the thermal stability, would result in a larger degradation rate. If $\frac{k_4}{k_{-4}} \ll 10^{-4}$, which is the case of homotrimer, the degradation rate is slow and is not sensitive to the thermal stability $\frac{k_4}{k_{-4}}$. While when $\frac{k_4}{k_{-4}}$ is large ($\frac{k_4}{k_{-4}} > 10^{-4}$) as the case of the heterotrimer, the degradation rate is fast and is dependent on the thermal stability. We find that an increase in thermal stability slows down the degradation rate. Moreover, when the rate MMP binds to vulnerable state is larger than it binds to the naive state $k_3 > k_1$, the degradation rate is more sensitive to the thermal stability. In summary, together with the atomistic simulations results, we find that the MMP resistance of homotrimer could be explained by the difference in thermal stability.

Force effects

We have shown that applied force stabilizes the heterotrimer. Therefore, it is clear (**Figure S1(b)**) that by decreasing $\frac{k_4}{k_{-4}}$, the applied force decreases the degradation rate. In contrast, for the homotrimer, applied force does not slow down the degradation by improving the thermal stability of homotrimer because the degradation rate of the homotrimer is not sensitive to the thermal stability when $\frac{k_4}{k_{-4}} \ll 1$ as shown in **Figure S1(b)**. It can be also seen from Eq. S4 that the degradation rate of the homotrimer is not dependent to the thermal stability.

Specificity, k_{cat}/K_m, calculations

Previously published data for the enzymatic degradation, using MMP-8, of reconstituted type I bovine collagen fibrils [9] was analyzed to extract specificity data for comparison in this manuscript. The solution to the reaction-diffusion equations governing the enzymatic erosion of insoluble collagen fibrils has been established for several limiting cases of enzyme and substrate concentrations [10]. For low enzyme and substrate concentrations, the condition met by the experiments described by Flynn et al, the collagen degradation rate is

$$\frac{d\rho(t)}{dt} = \frac{-k_{cat} E_o k \rho(t)^{1/2}}{K_m} \qquad [S7]$$

where ρ, E_o, k, k_{cat} and K_m are collagen concentration, initial enzyme concentration, fibril sizing parameter, molecular cleavage rate and Michaelis-Menten constant (Eq. 112, [10]). Rearranging Eq. S7 to

$$\frac{k_{cat}}{K_m} = -\frac{d\rho(t)}{dt}\frac{1}{E_o k \rho(t)^{1/2}} \qquad [S8]$$

yields an expression for specificity that is dependent upon the collagen concentration rate. The other parameters are known and constant for the experimental series. The collagen concentration is extracted from the observed fibril network edge intensity, which was shown to be linearly related to the mean network fibril diameter [9]. Specifically, a 50% drop in normalized integrated fibril edge intensity, from 0.9 to 0.4, represents a ~50% drop in mean fibril diameter, or a ~75% drop in bulk

collagen concentration. Time points at 0.9 and 0.2 normalized integrated network edge intensity were used for rate calculations (see figure 3 in [9]).

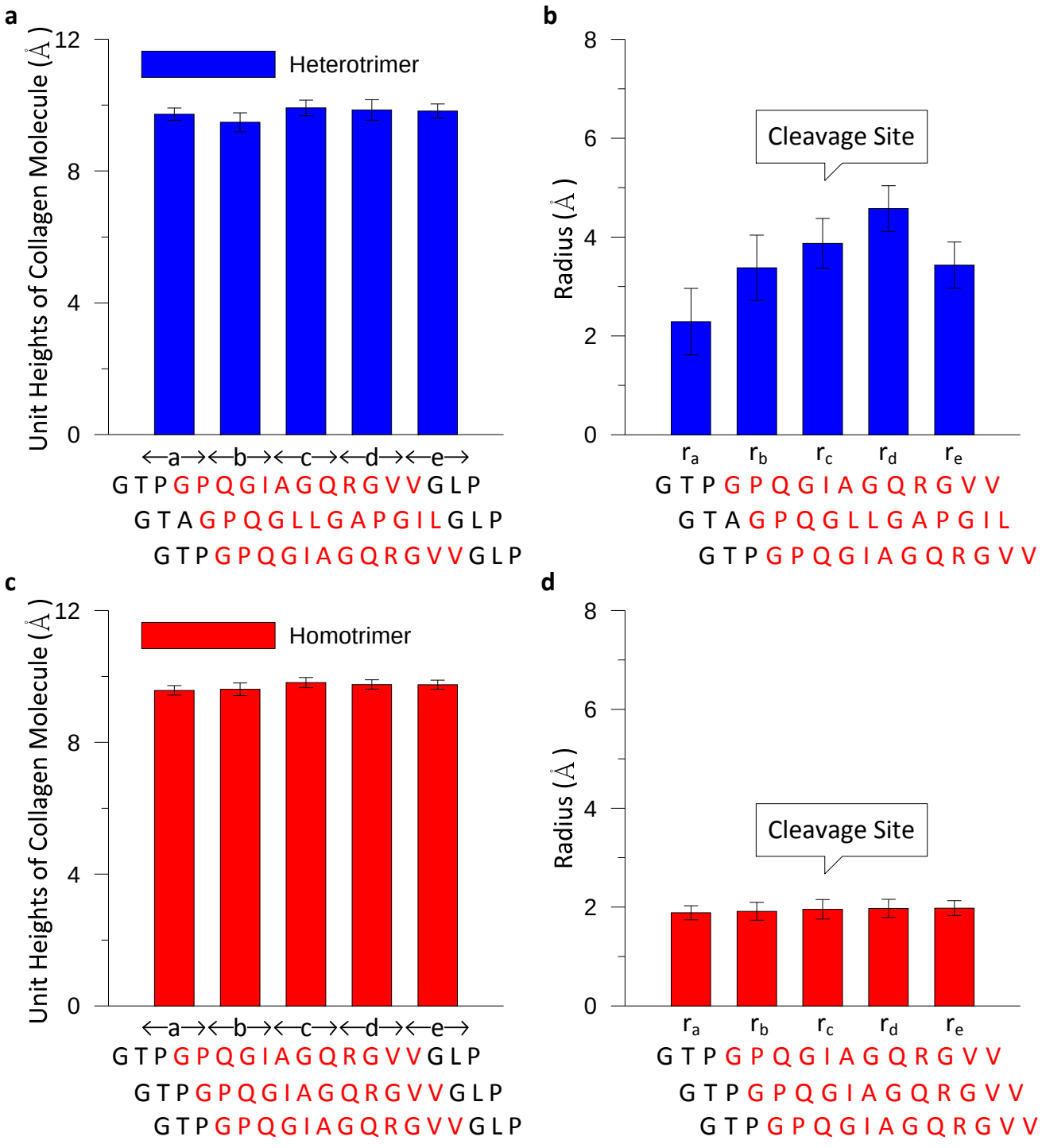

Figure S2 | Structural analyses of the vicinity of cleavage site of type I mouse heterotrimer and homotrimer with constant force applied. (a) The unit heights of heterotrimer at the vicinity of the cleavage site. (b) The radii of heterotrimer at the vicinity of the cleavage site. (c) The unit heights of homotrimer at the vicinity of the cleavage site. (d) The radii of homotrimer at the vicinity of the cleavage site.

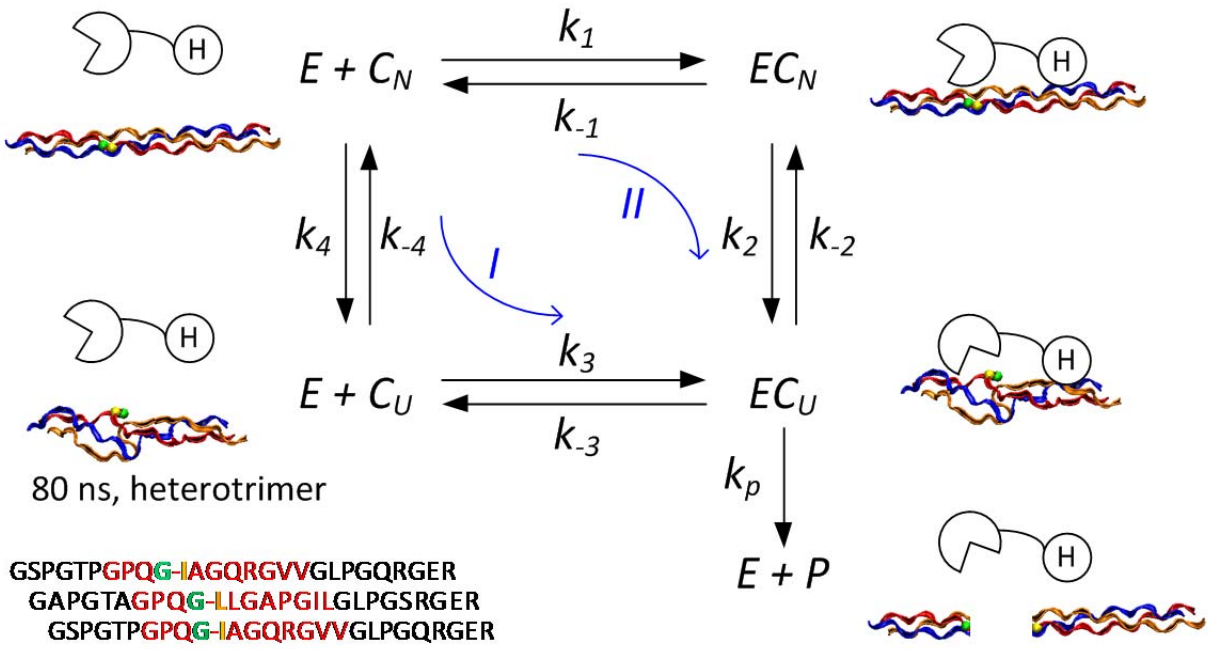

Figure S3 | Possible cleavage mechanisms of collagen molecules. There are two widely used models to explain the cleavage mechanism of collagen. In the first one, path I, collagen is thermally unfolded to a vulnerable state before the MMP binds to the collagen molecule [6]. The other one, path II, MMP binds to and unwinds the collagen molecule before cutting it [11]. Our results show that the heterotrimer is thermally unfolded at the cleavage site within 80 ns, indicating that it primarily goes path I. Mechanical tests reveal that the force stabilizes the cleavage site of the heterotrimer by refolding it into a triple helical structure and thus protects against enzymatic breakdown.

Supplementary references

[1] Han S, Makareeva E, Kuznetsova NV, DeRidder AM, Sutter MB, Losert W, et al. Molecular mechanism of type I collagen homotrimer resistance to mammalian collagenases. J Biol Chem. 2010;285:22276-81.
[2] Ottl J, Gabriel D, Murphy G, Knauper V, Tominaga Y, Nagase H, et al. Recognition and catabolism of synthetic heterotrimeric collagen peptides by matrix metalloproteinases. Chem Biol. 2000;7:119-32.
[3] Stultz CM, Nerenberg PS, Salsas-Escat R. Do collagenases unwind triple-helical collagen before peptide bond hydrolysis? Reinterpreting experimental observations with mathematical models. Proteins-Structure Function and Bioinformatics. 2008;70:1154-61.
[4] Salsas-Escat R, Nerenberg PS, Stultz CM. Cleavage site specificity and conformational selection in type I collagen degradation. Biochemistry. 2010;49:4147-58.
[5] Fields GB, Van Wart HE, Birkedal-Hansen H. Sequence specificity of human skin fibroblast collagenase. Evidence for the role of collagen structure in determining the collagenase cleavage site. J Biol Chem. 1987;262:6221-6.
[6] Stultz CM. Localized unfolding of collagen explains collagenase cleavage near imino-poor sites. J Mol Biol. 2002;319:997-1003.
[7] Xiao J, Addabbo RM, Lauer JL, Fields GB, Baum J. Local conformation and dynamics of isoleucine in the collagenase cleavage site provide a recognition signal for matrix metalloproteinases. J Biol Chem. 2010;285:34181-90.
[8] Salsas-Escat R, Stultz CM. Conformational selection and collagenolysis in type III collagen. Proteins. 2010;78:325-35.
[9] Flynn BP, Bhole AP, Saeidi N, Liles M, Dimarzio CA, Ruberti JW. Mechanical strain stabilizes reconstituted collagen fibrils against enzymatic degradation by mammalian collagenase matrix metalloproteinase 8 (MMP-8). PLoS One. 2010;5:e12337.
[10] Tzafriri AR, Bercovier M, Parnas H. Reaction diffusion model of the enzymatic erosion of insoluble fibrillar matrices. Biophysical Journal. 2002;83:776-93.
[11] Chung L, Dinakarpandian D, Yoshida N, Lauer-Fields JL, Fields GB, Visse R, et al. Collagenase unwinds triple-helical collagen prior to peptide bond hydrolysis. EMBO J. 2004;23:3020-30.